Available online at www.sciencedirect.com
ScienceDirect
Journal of Hazardous Materials 154 (2008) 337–346
Journal of Hazardous Materials
www.elsevier.com/locate/jhazmat

Adsorption of basic dye on high-surface-area activated carbon prepared from coconut husk: Equilibrium, kinetic and thermodynamic studies

I.A.W. Tan, A.L. Ahmad, B.H. Hameed *

School of Chemical Engineering, Universiti Sains Malaysia, Engineering Campus, 14300 Nibong Tebal, Penang, Malaysia

Received 21 August 2007; received in revised form 5 October 2007; accepted 8 October 2007
Available online 13 October 2007

Abstract

Adsorption isotherm and kinetics of methylene blue on activated carbon prepared from coconut husk were determined from batch tests. The effects of contact time (1–30 h), initial dye concentration (50–500 mg/l) and solution temperature (30–50 °C) were investigated. Equilibrium data were fitted to Langmuir, Freundlich, Temkin and Dubinin–Radushkevich isotherm models. The equilibrium data were best represented by Langmuir isotherm model, showing maximum monolayer adsorption capacity of 434.78 mg/g. The kinetic data were fitted to pseudo-first-order, pseudo-second-order and intraparticle diffusion models, and was found to follow closely the pseudo-second-order kinetic model. Thermodynamic parameters such as standard enthalpy (ΔH°), standard entropy (ΔS°) and standard free energy (ΔG°) were evaluated. The adsorption interaction was found to be exothermic in nature. Coconut husk-based activated carbon was shown to be a promising adsorbent for removal of methylene blue from aqueous solutions.

Keywords: Coconut husk activated carbon; Basic dye; Adsorption isotherm; Equilibrium; Kinetics

1. Introduction

The presence of dyes in effluents is a major concern due to their adverse effect to many forms of life. The discharge of dyes in the environment is worrying for both toxicological and esthetical reasons [1]. Industries such as textile, leather, paper, plastics, etc., are some of the sources for dye effluents [2]. It is estimated that more than 100,000 commercially available dyes with over 7×10^5 tonnes of dyestuff produced annually [3]. Methylene blue (MB) is the most commonly used substance for dying cotton, wood and silk. MB can cause eye burns which may be responsible for permanent injury to the eyes of human and animals. On inhalation, it can give rise to short periods of rapid or difficult breathing while ingestion through the mouth produces a burning sensation and may cause nausea, vomiting, profuse sweating, mental confusion and methemoglobinemia [4]. Therefore, the treatment of effluent containing such dye is of interest due to its harmful impacts on receiving waters.

Among several chemical and physical methods, the adsorption has been found to be superior compared to other techniques for wastewater treatment in terms of its capability for efficiently adsorbing a broad range of adsorbates and its simplicity of design. Colour removal from industrial wastewaters by adsorption techniques has been of growing importance due to the chemical and biological stability of dyestuffs to conventional water treatment methods and the growing need for high quality treatment [5]. However, commercially available activated carbons are still considered as expensive materials for many countries due to the use of non-renewable and relatively expensive starting material such as coal, which is unjustified in pollution control applications [6,7]. Therefore, in recent years, this has prompted a growing research interest in the production of activated carbons from renewable and cheaper precursors which are mainly industrial and agricultural by-products, such as apricot shell [8], male flower of coconut tree [9], jute fiber [10], rubber wood sawdust [11,12], corncob [13], bamboo [14] and oil palm fibre [15].

Coconut husk is the mesocarp of coconut and a coconut consists of 33–35% of husk. In Malaysia, about 151,000 ha of land was being used for coconut plantation in year 2001. It was estimated that 5280 kg of dry husks will become available per

* Corresponding author. Fax: +60 4594 1013.
E-mail address: chbassim@eng.usm.my (B.H. Hameed).

0304-3894/$ – see front matter © 2007 Elsevier B.V. All rights reserved.
doi:10.1016/j.jhazmat.2007.10.031

hectare per year. At present, coconut husks are used as fuel for coconut processing, as a domestic fuel and as a source of fibre for rope and mats [16].

To make better use of this cheap and abundant agricultural waste, it is proposed to convert coconut husk into activated carbon. Conversion of coconut husk to activated carbon will serve a double purpose. First, unwanted agricultural waste is converted to useful, value-added adsorbent and second, the use of agricultural by-products represents a potential source of adsorbents which will contribute to solving part of the wastewater treatment problem in Malaysia. However, not many studies have been done on converting coconut husk to activated carbon. Some of them are adsorption of arsenic on copper impregnated coconut husk carbon [17] and the preparation of activated carbon from digested sewage sludge with the additive coconut husk using $ZnCl_2$ as activating agent which reported that the highest BET surface area obtained was 867.61 m^2/g [18].

Adsorption of dyes from aqueous solution requires activated carbons possessing not only large capacities, but also significant pore volumes and surface areas contributed by mesopores, due to the size of dye molecules which are relatively large. The focus of this research was to evaluate the adsorption potential of the coconut husk-based activated carbon in removing MB from aqueous solutions. Textural characterization of the prepared activated carbon was also carried out. The equilibrium, kinetic and thermodynamic data of the adsorption process were then evaluated to study the adsorption mechanism of MB molecules onto the prepared activated carbon.

2. Materials and methods

2.1. Preparation and characterization of activated carbon

Coconut husk used for preparation of activated carbon was obtained locally. The precursor was first washed with distilled water, dried, cut and sieved to desired mesh size of 1–2 mm. Then, it was carbonized and activated following the same procedure used in our previous study on activated carbon preparation from oil palm fibre [15], where the precursor was carbonized in a stainless steel vertical tubular reactor placed in a tube furnace under purified nitrogen (99.995%) flow of 150 cm^3/min at 700 °C, with heating rate of 10 °C/min and the sample was hold at the carbonization temperature for 2 h. The char produced was soaked in potassium hydroxide (KOH) solution with KOH:char ratio of 1:1 (w/w). The mixture was then dehydrated in an oven overnight at 105 °C to remove moisture and then activated under the same condition as carbonization, but to a final temperature of 850 °C. Once the final temperature was reached, the nitrogen gas flow was switched to carbon dioxide (CO_2) and activation was held for 2 h. The activated product was then cooled under nitrogen gas flow to room temperature and then washed with hot deionized water and 0.1 M hydrochloric acid until the pH of the washing solution reached 6–7.

Textural characterization of the prepared activated carbon was carried out by N_2 adsorption at 77 K using Autosorb I (Quantachrome Corporation, USA). The Brunauer–Emmett–Teller (BET) surface area, total pore volume and pore size distribution of the prepared activated carbon were then determined [19,20]. Scanning electron microscopy (SEM) analysis was carried out for the precursor and the prepared activated carbon to study their surface textures and the development of porosity.

2.2. Batch equilibrium studies

MB supplied by Sigma–Aldrich (M) Sdn Bhd, Malaysia was used as an adsorbate and was not purified prior to use. Deionized water was used to prepare all the solutions and reagents. MB was chosen in this study due to its wide application and known strong adsorption onto solids. MB has a chemical formula of $C_{16}H_{18}N_3SCl$, with molecular weight of 319.86 g/mol, which corresponds to methylene blue hydrochloride with three groups of water. Chemical structure of MB is shown in Appendix A.

Adsorption tests were performed in a set of 43 Erlenmeyer flasks (250 ml) where 100 ml of methylene blue solutions with initial concentrations of 50–500 mg/l were placed in these flasks. Equal mass of 0.10 g of the prepared activated carbon with particle size of 200 μm was added to each flask and kept in an isothermal shaker of 120 rpm at 30 °C for 30 h to reach equilibrium. The pH of the solutions was original without any pH adjustment. Similar procedures were followed for another two sets of Erlenmeyer flask containing the same initial dye concentrations and same activated carbons dosage, but were kept under 40 and 50 °C for thermodynamic studies. Aqueous samples were taken from each of the MB solutions at preset time intervals using disposable syringes and the concentrations were then analyzed. All samples were filtered prior to analysis in order to minimize interference of the carbon fines with the analysis. The concentrations of MB in the supernatant solution before and after adsorption were determined using a double beam UV–visible spectrophotometer (UV-1601 Shimadzu, Japan) at 668 nm. Each experiment was duplicated under identical conditions. The amount of adsorption at equilibrium, q_e (mg/g), was calculated by:

$$q_e = \frac{(C_0 - C_e)V}{W} \quad (1)$$

where C_0 and C_e (mg/l) are the liquid-phase concentrations of dye initially and at equilibrium, respectively. V is the volume of the solution (l) and W is the mass of dry adsorbent used (g).

The equilibrium data were then fitted using four different isotherm models, namely the Langmuir, Freundlich, Temkin and Dubinin–Radushkevich models.

2.2.1. Langmuir isotherm

Langmuir isotherm assumes monolayer adsorption onto a surface containing a finite number of adsorption sites of uniform strategies of adsorption with no transmigration of adsorbate in the plane of surface [21]. The linear form of Langmuir isotherm equation is given as:

$$\frac{C_e}{q_e} = \frac{1}{Q_o b} + \frac{1}{Q_o} C_e \quad (2)$$

where C_e is the equilibrium concentration of the adsorbate (mg/l), q_e is the amount of adsorbate adsorbed per unit mass

of adsorbent (mg/g), Q_o and b are Langmuir constants related to adsorption capacity and rate of adsorption, respectively.

2.2.2. Freundlich isotherm

Freundlich isotherm in the other hand assumes heterogeneous surface energies, in which the energy term in Langmuir equation varies as a function of the surface coverage [21]. The well-known logarithmic form of the Freundlich isotherm is given by the following equation:

$$\log q_e = \log K_F + \left(\frac{1}{n}\right) \log C_e \tag{3}$$

where C_e is the equilibrium concentration of the adsorbate (mg/l), q_e is the amount of adsorbate adsorbed per unit mass of adsorbent (mg/g), K_F and n are Freundlich constants with n giving an indication of how favorable the adsorption process. K_F (mg/g (l/mg)$^{1/n}$) is the adsorption capacity of the adsorbent which can be defined as the adsorption or distribution coefficient and represents the quantity of dye adsorbed onto activated carbon for a unit equilibrium concentration. The slope of $1/n$ ranging between 0 and 1 is a measure of adsorption intensity or surface heterogeneity, becoming more heterogeneous as its value gets closer to zero [22]. A value for $1/n$ below one indicates a normal Langmuir isotherm while $1/n$ above one is indicative of cooperative adsorption [23].

2.2.3. Temkin isotherm

Temkin and Pyzhev considered the effects of indirect adsorbate/adsorbate interactions on adsorption isotherms. The heat of adsorption of all the molecules in the layer would decrease linearly with coverage due to adsorbate/adsorbate interactions [24]. The Temkin isotherm has been used in the form as follows:

$$q_e = \left(\frac{RT}{b}\right) \ln(AC_e) \tag{4}$$

where $RT/b = B$, R is the gas constant (8.31 J/mol K) and T (K) is the absolute temperature.

2.2.4. Dubinin–Radushkevich isotherm

Another popular equation for the analysis of isotherms of a high degree of rectangularity is that proposed by Dubinin and Radushkevich as follow:

$$q_e = q_s \exp(-B\varepsilon^2) \tag{5}$$

where ε can be correlated:

$$\varepsilon = RT \ln\left[1 + \frac{1}{C_e}\right] \tag{6}$$

The constant B gives the mean free energy E of sorption per molecule of the sorbate when it is transferred to the surface of the solid from infinity in the solution and can be computed by using the relationship:

$$E = \frac{1}{\sqrt{2B}} \tag{7}$$

2.3. Batch kinetic studies

The procedure of kinetic tests was identical to those of equilibrium tests. The aqueous samples were taken at preset time intervals and the concentrations of MB were similarly measured. The amount of adsorption at time t, q_t (mg/g), was calculated by:

$$q_t = \frac{(C_0 - C_t)V}{W} \tag{8}$$

where C_t (mg/l) is the liquid-phase concentrations of dye at time, t.

The kinetic data were then fitted using the pseudo-first-order, pseudo-second-order and intraparticle diffusion models.

2.3.1. Pseudo-first-order kinetic model

The rate constant of adsorption is determined from the pseudo-first-order equation given by Langergren and Svenska [25] as:

$$\ln(q_e - q_t) = \ln q_e - k_1 t \tag{9}$$

where q_e and q_t are the amounts of MB adsorbed (mg/g) at equilibrium and at time t (h), respectively and k_1 is the rate constant adsorption (h^{-1}).

2.3.2. Pseudo-second-order kinetic model

The pseudo-second-order equation [26] based on equilibrium adsorption is expressed as:

$$\frac{t}{q_t} = \frac{1}{k_2 q_e^2} + \frac{1}{q_e} t \tag{10}$$

where k_2 (g/mg h) is the rate constant of second-order adsorption.

2.3.3. Intraparticle diffusion model

Intraparticle diffusion model based on the theory proposed by Weber and Morris [27] was tested to identify the diffusion mechanism. It is an empirically found functional relationship, common to the most adsorption processes, where uptake varies almost proportionally with $t^{1/2}$ rather than with the contact time t. According to this theory:

$$q_t = k_p t^{1/2} + C \tag{11}$$

where k_p (mg/g h$^{1/2}$) is the intraparticle diffusion rate constant.

2.3.4. Validity of kinetic model

The applicability of the kinetic model to describe the adsorption process was further validated by the normalized standard deviation, Δq (%), which is defined as:

$$\Delta q\,(\%) = 100\sqrt{\frac{\sum[(q_{exp} - q_{cal})/q_{exp}]^2}{N-1}} \tag{12}$$

where N is the number of data points, q_{exp} and q_{cal} (mg/g) are the experimental and calculated adsorption capacity, respectively.

2.4. Adsorption thermodynamics

The thermodynamic parameters that must be considered to determine the process are changes in standard enthalpy (ΔH°), standard entropy (ΔS°) and standard free energy (ΔG°) due to transfer of unit mole of solute from solution onto the solid–liquid interface. The value of ΔH° and ΔS° were computed using the following equation:

$$\ln K_d = \frac{\Delta S^\circ}{R} - \frac{\Delta H^\circ}{RT} \quad (13)$$

where R (8.314 J/mol K) is the universal gas constant, T (K) is the absolute solution temperature and K_d is the distribution coefficient which can be calculated as:

$$K_d = \frac{C_{Ae}}{C_e} \quad (14)$$

where C_{Ae} (mg/l) is the amount adsorbed on solid at equilibrium and C_e (mg/l) is the equilibrium concentration.

ΔG° can be calculated using the relation below:

$$\Delta G^\circ = -RT \ln K_d \quad (15)$$

3. Results and discussion

3.1. Textural characterization of prepared activated carbon

The BET surface area of the prepared activated carbon was found to be 1940 m^2/g, with total pore volume of 1.143 cm^3/g. The pore size distribution of the prepared activated carbon is shown in Fig. 1. A few peaks were detected, with the sharpest peak occurred at pore diameter between 3 and 4 nm and the average pore diameter of the prepared sample was found to be 2.36 nm. This indicated that the activated carbon derived from coconut husk was mesoporous, with relatively large surface area and total pore volume compared to commercially available activated carbons such as BDH from Merck, F100 and BPL from Calgon Corp. with BET surface area of 1118, 957 and 972 m^2/g as well as total pore volume of 0.618, 0.526 and 0.525 cm^3/g, respectively [20]. Stavropoulos and Zabaniotou [20] stated that KOH is dehydrated to K_2O, which reacts with CO_2 produced by the water-shift reaction, to give K_2CO_3. Intercalation of metallic

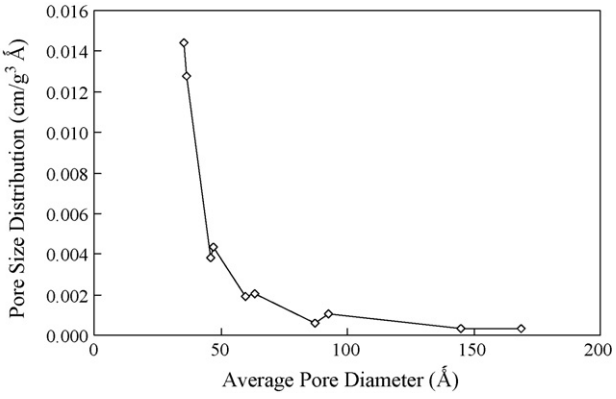

Fig. 1. Pore size distribution of prepared activated carbon.

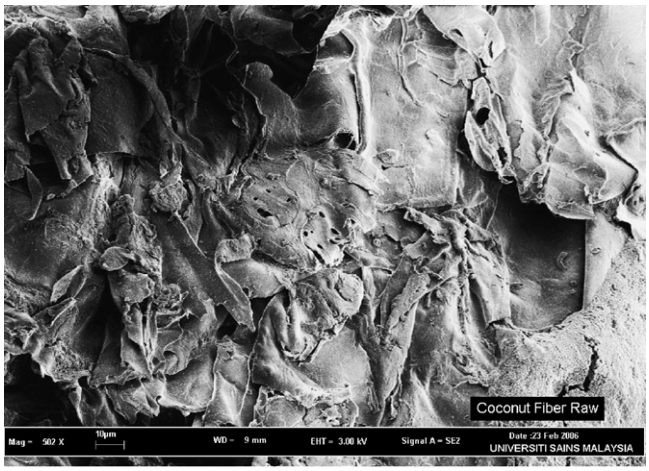

(a). SEM image of raw coconut husk (500x).

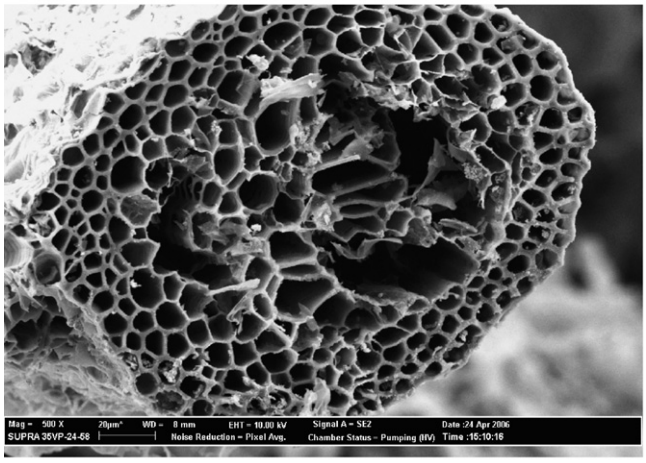

(b). SEM image of coconut husk-based activated carbon (500x).

Fig. 2. SEM image of: (a) raw coconut husk (500×) and (b) coconut husk-based activated carbon (500×).

potassium appeared to be responsible for the drastic expansion of the carbon material and hence the creation of a large specific surface area and high pore volume. Similar observation was reported by Tseng et al. [13] where CO_2 gasification was found to promote the formation of mesopores and enhance the surface area of activated carbon.

Fig. 2(a and b) shows the SEM images of the precursor and the derived activated carbon, respectively. Many large pores in a honeycomb shape were clearly found on the surface of the activated carbon, as compared to the precursor. This shows that KOH and CO_2 were effective in creating well-developed pores on the surface of the precursor, hence leading to the activated carbon with large surface area and porous structure.

3.2. Effect of contact time and initial dye concentration on adsorption equilibrium

Fig. 3 shows the adsorption capacity versus the adsorption time at various initial MB concentrations. It indicated that the contact time needed for MB solutions with initial concentrations of 50–300 mg/l to reach equilibrium was around 2 h. However, for MB solutions with higher initial concentrations of

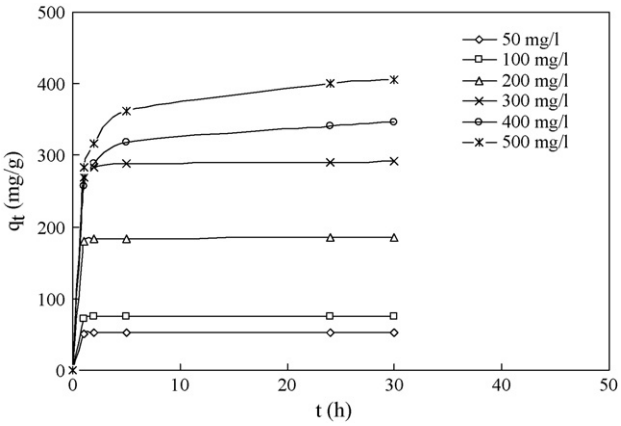

Fig. 3. Adsorption capacity versus adsorption time at various initial methylene blue concentrations at 30 °C.

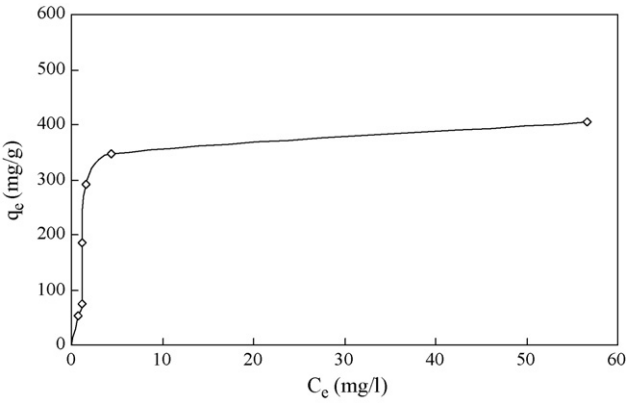

Fig. 4. Equilibrium adsorption isotherm of methylene blue onto prepared activated carbon at 30 °C.

400–500 mg/l, equilibrium times of around 30 h were required. This observation could be explained by the theory that in the process of dye adsorption, initially the dye molecules have to first encounter the boundary layer effect and then diffuse from the boundary layer film onto adsorbent surface and then finally, they have to diffuse into the porous structure of the adsorbent [10,28]. Therefore, MB solutions of higher initial concentrations will take relatively longer contact time to attain equilibrium due to higher amount of dye molecules. Similar phenomenon was observed for the adsorption of MB from aqueous solution on jute fiber carbon where the equilibrium time was found to be 250 min [10].

As can be seen from Fig. 3, the amount of MB adsorbed on the activated carbon increases with time and, at some point in time, it reaches a constant value beyond which no more MB is further removed from the solution. At this point, the amount of the dye desorbing from the activated carbon is in a state of dynamic equilibrium with the amount of the dye being adsorbed on the activated carbon. The amount of dye adsorbed at the equilibrium time reflects the maximum adsorption capacity of the adsorbent under those operating conditions. In this study, the adsorption capacity at equilibrium (q_e) increased from 52 to 405 mg/g with an increase in the initial dye concentrations from 50 to 500 mg/l. When the initial concentration increased, the mass transfer driving force would become larger, hence resulting in higher adsorption of MB.

3.3. Adsorption isotherms

The adsorption isotherm indicates how the adsorption molecules distribute between the liquid phase and the solid phase when the adsorption process reaches an equilibrium state. The analysis of the isotherm data by fitting them to different isotherm models is an important step to find the suitable model that can be used for design purposes [29]. Adsorption isotherm is basically important to describe how solutes interact with adsorbents, and is critical in optimizing the use of adsorbents. Fig. 4 shows the equilibrium adsorption isotherm of MB on the prepared activated carbon. It exhibits a steep increase at low concentrations, indicating high affinity towards the solute. At high MB concentrations, the adsorbed amounts increase slightly, showing almost horizontal plateaus.

Adsorption isotherm study was carried out on four isotherm models: the Langmuir, Freundlich, Temkin and Dubinin–Radushkevich isotherm models. The applicability of the isotherm equation to describe the adsorption process was judged by the correlation coefficients, R^2 values. For the Langmuir isotherm, when C_e/q_e is plotted against C_e, a straight line with slope of $1/Q_o$ is obtained, as shown in Fig. 5. The correlation coefficient, R^2 of 0.99 indicated that the adsorption data of MB on the prepared activated carbon was well fitted to the Langmuir isotherm. The Langmuir constants b and Q_o were calculated from Eq. (2) and are shown in Table 1.

The essential characteristics of the Langmuir isotherm can be expressed in terms of a dimensionless equilibrium parameter (R_L) [21]. The parameter is defined by:

$$R_L = \frac{1}{1 + bC_0} \tag{16}$$

where b is the Langmuir constant and C_0 is the highest initial dye concentration (mg/l). The value of R_L indicates the type of the isotherm to be either unfavorable ($R_L > 1$), linear ($R_L = 1$),

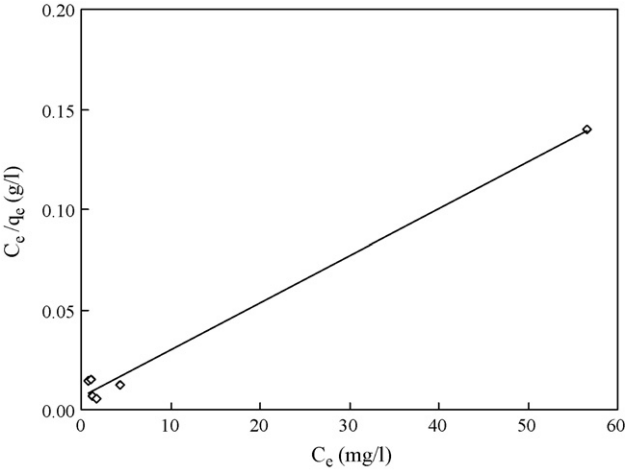

Fig. 5. Langmuir adsorption isotherm of methylene blue onto prepared activated carbon at 30 °C.

Table 1
Langmuir, Freundlich, Temkin and Dubinin–Radushkevich isotherm model parameters and correlation coefficients for adsorption of MB on prepared activated carbon

Isotherms	Solution temperature (K)	Parameters		R^2
Langmuir		Q_o (mg/g)	b (l/mg)	
	303	434.78	0.34	0.99
	313	416.67	4.00	0.99
	323	384.62	5.20	1.00
Freundlich		K_F (mg/g(l/mg)$^{1/n}$)	$1/n$	
	303	120.17	0.38	0.51
	313	238.29	0.15	0.48
	323	209.41	0.19	0.74
Temkin		A (l/g)	B	
	303	7.45	74.90	0.68
	313	6726.94	32.66	0.71
	323	1745.74	34.58	0.92
Dubinin–Radushkevich		q_s (mg/g)	E	
	303	423.73	1000.00	0.87
	313	386.45	7071.07	0.49
	323	359.03	7071.07	0.83

favorable ($0 < R_L < 1$) or irreversible ($R_L = 0$). Value of R_L was found to be 0.006, 0.0005 and 0.0004, respectively at solution temperature of 30, 40 and 50 °C. This again confirmed that the Langmuir isotherm was favorable for adsorption of MB on the activated carbon under the conditions used in this study.

For the Freundlich isotherm, the plot of log q_e versus log C_e gives a straight line with slope of $1/n$ with value of 0.38, as shown in Fig. 6, which showed that the adsorption of MB on the activated carbon was favorable. Accordingly, Freundlich constants K_F and n were calculated from Eq. (3) and are listed in Table 1. A plot of q_e versus ln C_e for the Temkin isotherm yields a linear line, as shown in Fig. 7. The constants A and B are shown in Table 1. For Dubinin–Radushkevich isotherm, a plot of ln q_e versus ε^2 (Fig. 8) enables the constants q_s and E to be determined (Table 1).

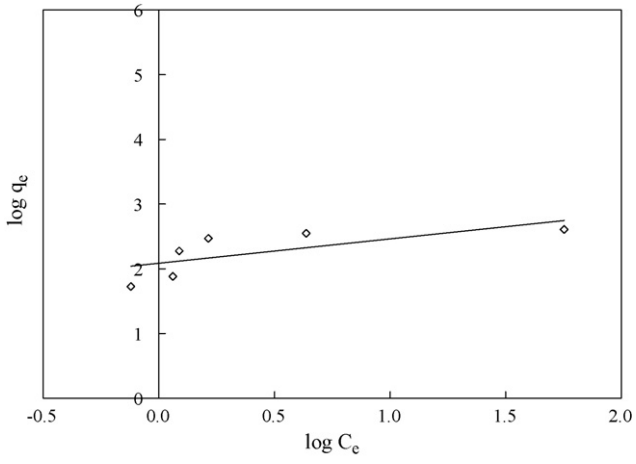

Fig. 6. Freundlich adsorption isotherm of methylene blue onto prepared activated carbon at 30 °C.

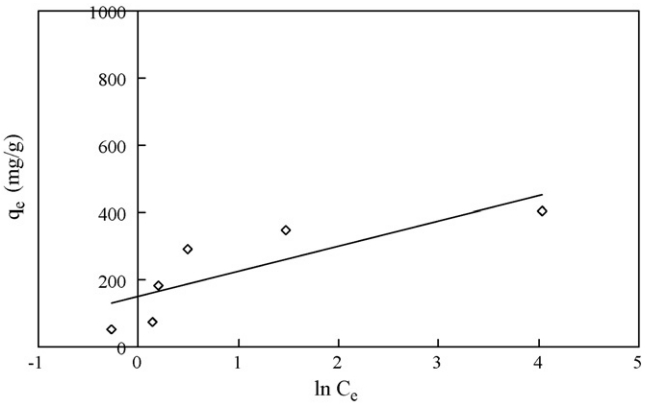

Fig. 7. Temkin adsorption isotherm of methylene blue onto prepared activated carbon at 30 °C.

Table 1 summarizes all the constants and correlation coefficients, R^2 of the four isotherm models used. The Langmuir model yielded the best fit with R^2 values equal or higher than 0.99, as compared to the other three models. Conformation of the experimental data into Langmuir isotherm equation indicated the homogeneous nature of coconut husk-based activated carbon surface, i.e., each dye molecule/coconut husk carbon adsorption had equal adsorption activation energy. The results also demonstrated the formation of monolayer coverage of dye molecule at the outer surface of coconut husk activated carbon. Similar observations were reported by the adsorption of MB on activated carbons prepared from jute fiber [10], olive-seed waste residue [20] and corncob [13].

Table 2 lists the comparison of maximum monolayer adsorption capacity of MB using various adsorbents. The activated carbon prepared in this work had a relatively large adsorption capacity of 434.78 mg/g if compared to some data obtained from the literature. The high adsorption capacity of the activated carbon prepared in this study could be due to its relatively high surface area and its mesoporous structure. The variation in the adsorption capacity compared to other adsorbents as listed is Table 2, might be due to the variation in the original nature of the precursors, the processes applied to produce the adsorbents as well as the conditions used during the adsorption processes.

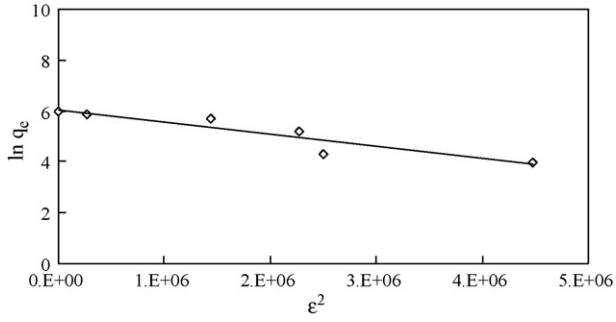

Fig. 8. Dubinin–Radushkevich adsorption isotherm of methylene blue onto prepared activated carbon at 30 °C.

Table 2
Comparison of the maximum monolayer adsorption of MB on various adsorbents

Adsorbents	Maximum monolayer adsorption capacity (mg/g)	References
Coconut husk-based activated carbon	434.78	This work
Bamboo dust-based activated carbon	143.20	[35]
Coconut shell-based activated carbon	277.90	[35]
Groundnut shell-based activated carbon	164.90	[35]
Oil palm fibre-based activated carbon	277.78	[15]
Jute fiber-based activated carbon	225.64	[10]
Mango seed kernel powder	142.86	[4]
Waste apricot-based activated carbon	102.04–136.98	[5]
Coir pith carbon	5.87	[31]
Olive-seed waste residue-based activated carbon	190.00–263.00	[20]
Filtrasorb F300[a]	240.00	[20]

[a] Commercial activated carbon.

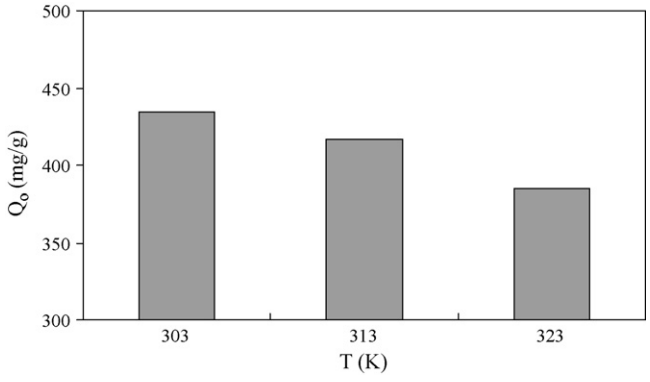

Fig. 9. Maximum monolayer adsorption capacity, Q_o, of MB on the prepared activated carbon versus temperature.

3.4. Effect of temperature on adsorption capacity of activated carbon

Fig. 9 shows the maximum monolayer adsorption capacity, Q_o, of MB on the prepared activated carbon versus the temperature. It was found that the adsorption capacity decreased from 434.78 to 384.62 mg/g with increase in temperature from 30 to 50 °C, indicating the exothermic nature of the adsorption reaction. Similar trend was reported by Chandra et al. [30] for adsorption of MB on activated carbon prepared from durian shell. It was explained that as temperature increased, the physical bonding between the organic compounds (including dyes) and the active sites of the adsorbent weakened. Besides, the solubility of MB also increased which caused the interaction forces between the solute and the solvent to become stronger than solute and adsorbent, therefore the solute was more difficult to adsorb.

3.5. Adsorption kinetics

Values of k_1 for the pseudo-first-order kinetic model were obtained from the slopes of the linear plots of $\ln(q_e - q_t)$ versus t (figure not shown). The correlation coefficient values obtained were relatively small and the experimental q_e values did not agree with the calculated values obtained from the linear plots, as shown in Table 3. This shows that the adsorption of MB onto the activated carbon did not follow the pseudo-first-order equation.

If the pseudo-second-order kinetic model is applicable, the plot of t/q_t versus t should show a linear relationship. q_e and k_2 can then be determined from the slope and the intercept of the plot. This procedure is more likely to predict the behavior over the whole range of adsorption. The linear plot of t/q_t versus t, as shown in Fig. 10, shows a good agreement between the experimental and the calculated q_e values (Table 3). Besides, the correlation coefficients for the second-order kinetic model were greater than 0.99 for all MB concentrations, indicating the applicability of the second-order kinetic model to describe the adsorption process of MB on the prepared activated carbon.

The intraparticle diffusion model rate constant, K_p is obtained from the slope of the straight line of q_t versus $t^{1/2}$ (Fig. 11). Values of intercept, C, give an idea about the thickness of boundary layer, i.e., larger the intercept, greater is the boundary layer effect [31]. The R^2 values (Table 4) obtained were lower compared to those obtained from pseudo-second-order

Table 3
Pseudo-first-order and pseudo-second-order kinetic model parameters for different initial MB concentrations at 30 °C

Initial MB concentration (mg/l)	$q_{e,exp}$ (mg/g)	Pseudo-first-order kinetic model				Pseudo-second-order kinetic model			
		$q_{e,cal}$ (mg/g)	k_1 (h)	R^2	Δq (%)	$q_{e,cal}$ (mg/g)	k_2 (g/g h)	R^2	Δq (%)
50	52.78	2.26	0.07	0.18	134.28	52.91	0.595	1.000	1.02
100	75.36	1.74	0.08	0.14	93.52	75.19	0.590	1.000	1.02
200	184.52	2.20	0.09	0.15	75.20	185.19	0.486	1.000	0.74
300	291.85	30.52	0.12	0.61	86.88	294.12	0.039	1.000	0.65
400	346.44	122.13	0.15	0.90	105.19	344.83	0.006	0.999	3.62
500	405.30	172.07	0.16	0.94	112.11	416.67	0.004	0.999	3.73

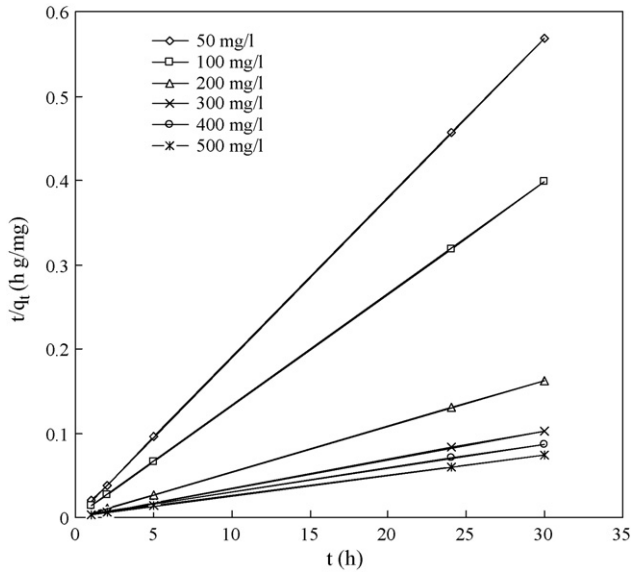

Fig. 10. Pseudo-second-order kinetics for adsorption of methylene blue onto prepared activated carbon at 30 °C.

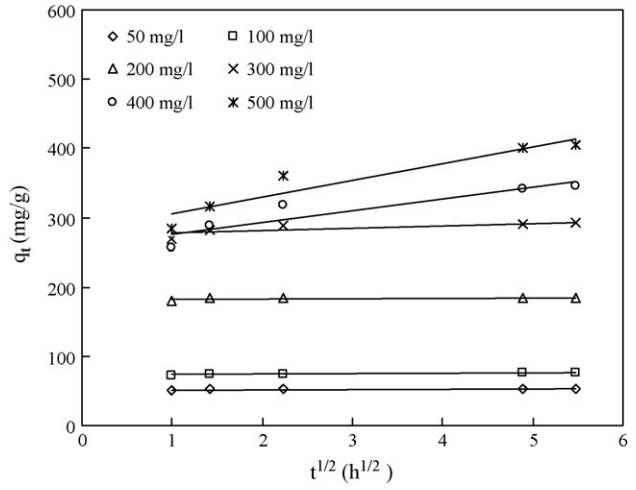

Fig. 11. Intraparticle diffusion model for adsorption of MB onto activated carbon at 30 °C.

kinetic model, however, the calculated and experimental q_e values agreed satisfactorily well for intraparticle diffusion model. The first, sharper portion is the instantaneous adsorption or external surface adsorption. The second portion is the gradual adsorption stage where intraparticle diffusion is the rate limiting. In some cases, the third portion exists, which is the final equilibrium stage where intraparticle diffusion starts to slow down due to the extremely low adsorbate concentrations left in the solutions [32]. As can be seen from Fig. 11, the linear line did not pass through the origin and this deviation from the origin or near saturation might be due to the difference in the mass transfer rate in the initial and final stages of adsorption [33].

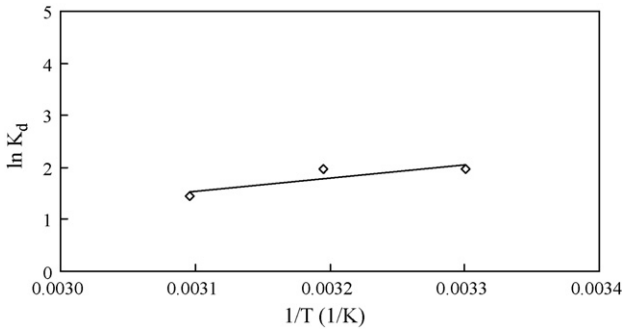

Fig. 12. Plot of ln K_d versus $1/T$ for 500 mg/l initial MB concentration.

Tables 3 and 4 list the Δq values obtained for the three models tested. The pseudo-second-order kinetic model yielded the lowest Δq values which ranged between 0.65 and 3.73% for MB initial concentration ranging from 50 to 500 mg/l. Based on the highest R^2 values which approached unity and the lowest Δq value, the pseudo-second-order model was the most suitable equation to describe the adsorption kinetics of MB on the prepared activated carbon. This suggested that the overall rate of the adsorption process was controlled by chemisorption which involved valency forces through sharing or exchange of electrons between the sorbent and sorbate [34]. The results were in agreement with the previous works on adsorption of MB on activated carbons prepared from bamboo [14] and oil palm fibre [15].

3.6. Adsorption thermodynamics

The values of ΔH° and ΔS° were calculated from the slope and intercept of plot between ln K_d versus $1/T$ for initial MB concentration of 500 mg/l (Fig. 12). The calculated values of ΔH°, ΔS° and ΔG° are listed in Table 5. The negative value of ΔH° indicated the exothermic nature of the adsorption interaction.

Table 4
Intraparticle diffusion model parameters for different initial MB concentrations at 30 °C

Initial MB concentration (mg/l)	Intraparticle diffusion model				
	$q_{e,cal}$ (mg/g)	k_p (mg/g h$^{1/2}$)	C	R^2	Δq (%)
50	52.93	0.33	51.12	0.40	1.43
100	75.63	0.39	73.49	0.33	1.37
200	184.90	0.51	182.10	0.32	0.75
300	293.19	3.61	273.42	0.61	1.91
400	351.39	16.71	259.84	0.85	4.53
500	413.52	24.29	280.46	0.89	4.77

Table 5
Thermodynamic parameters for adsorption of MB on prepared activated carbon

Initial concentration (mg/l)	ΔH° (J/mol)	ΔS° (J/mol K)	ΔG° (J/mol)		
			303 K	313 K	323 K
500	−20812.40	51.64	−4958.53	−5088.65	−3897.53

This decrease in adsorption capacity with increase in temperature is known to be due to the enhancement of the desorption step in the sorption mechanism. It is also due to the weakening of sorptive forces between the active sites on the activated carbon and the dye species, and also between adjacent dye molecules on the sorbed phase.

The positive value of ΔS° showed the affinity of the coconut husk-based activated carbon for MB and the increasing randomness at the solid–solution interface during the adsorption process. The negative value of ΔG° indicated the feasibility of the process and the spontaneous nature of the adsorption with a high preference of MB onto the prepared activated carbon. The values of ΔG° were found to decrease as the temperature increased, indicating less driving force and hence resulting in less adsorption capacity.

4. Conclusion

The present investigation showed that activated carbon prepared from coconut husk was a promising adsorbent for the removal of methylene blue dye from aqueous solutions over a wide range of concentrations. The surface area of the prepared activated carbon was relatively high with large pore volume and was found to be mesoporous. Methylene blue was found to adsorb strongly on the surface of the activated carbon. Equilibrium data were fitted to Langmuir, Freundlich, Temkin and Dubinin–Radushkevich isotherms and the equilibrium data were best described by the Langmuir isotherm model, with maximum monolayer adsorption capacity of 434.78 mg/g at 30 °C. The maximum monolayer adsorption capacity decreased with increasing temperature. The adsorption kinetics was found to follow closely the pseudo-second-order kinetic model. The negative ΔH° value confirmed the exothermic nature of the adsorption interaction whereas the positive ΔS° value showed the increased randomness at the solid–solution interface during the adsorption process. The negative value of ΔG° indicated the feasibility and the spontaneous nature of the adsorption of MB onto the prepared activated carbon. The adsorption performance of the coconut husk-based activated carbon was comparable to the commercial activated carbon and some other adsorbents reported in earlier studies.

Acknowledgment

The authors acknowledge the research grant provided by the Universiti Sains Malaysia under The Fundamental Research Grant Scheme (Project no.: 6070015).

Appendix A. Chemical structure of methylene blue dye

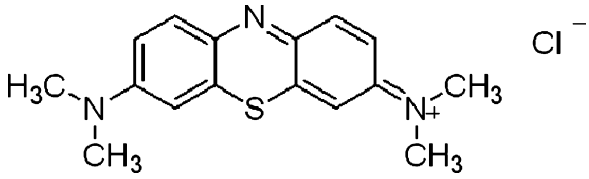

References

[1] H. Métivier-Pignon, C. Faur-Brasquet, P.L. Cloirec, Adsorption of dyes onto activated carbon cloths: approach of adsorption mechanisms and coupling of ACC with ultrafiltration to treat coloured wastewaters, Sep. Purif. Technol. 31 (2003) 3–11.
[2] K. Ravikumar, B. Deebika, K. Balu, Decolourization of aqueous dye solutions by a novel adsorbent: application of statistical designs and surface plots for the optimization and regression analysis, J. Hazard. Mater. B122 (2005) 75–83.
[3] J.W. Lee, S.P. Choi, R. Thiruvenkatachari, W.G. Shim, H. Moon, Evaluation of the performance of adsorption and coagulation processes for the maximum removal of reactive dyes, Dyes Pigments 69 (2006) 196–203.
[4] D. Ghosh, K.G. Bhattacharyya, Adsorption of methylene blue on kaolinite, Appl. Clay. Sci. 20 (2002) 295–300.
[5] C.A. Başar, Applicability of the various adsorption models of three dyes adsorption onto activated carbon prepared waste apricot, J. Hazard. Mater. B135 (2006) 232–241.
[6] A.A. Attia, B.S. Girgis, N.A. Fathy, Removal of methylene blue by carbons derived from peach stones by H_3PO_4 activation: batch and column studies, Dyes Pigments 76 (2008) 282–289.
[7] M.J. Martin, A. Artola, M.D. Balaguer, M. Rigola, Activated carbons developed from surplus sewage sludge for the removal of dyes from dilute aqueous solutions, Chem. Eng. J. 94 (2003) 231–239.
[8] B. Karagozoglu, M. Tasdemir, E. Demirbas, M. Kobya, The adsorption of basic dye (Astrazon Blue FGRL) from aqueous solutions onto sepiolite, fly ash and apricot shell activated carbon: kinetic and equilibrium studies, J. Hazard. Mater. 147 (2007) 297–306.
[9] S. Senthilkumaar, P. Kalaamani, C.V. Subburaam, Liquid phase adsorption of Crystal violet onto activated carbons derived from male flowers of coconut tree, J. Hazard. Mater. 136 (2006) 800–808.
[10] S. Senthilkumaar, P.R. Varadarajan, K. Porkodi, C.V. Subbhuraam, Adsorption of methylene blue onto jute fiber carbon: kinetics and equilibrium studies, J. Colloid Interface Sci. 284 (2005) 78–82.
[11] M.H. Kalavathy, T. Karthikeyan, S. Rajgopal, L.R. Miranda, Kinetic and isotherm studies of Cu(II) adsorption onto H_3PO_4-activated rubber wood sawdust, J. Colloid Interface Sci. 292 (2005) 354–362.
[12] B.G. Prakash Kumar, L.R. Miranda, M. Velan, Adsorption of Bismark Brown dye on activated carbons prepared from rubberwood sawdust (*Hevea brasiliensis*) using different activation methods, J. Hazard. Mater. B126 (2005) 63–70.
[13] R.L. Tseng, S.K. Tseng, F.C. Wu, Preparation of high surface area carbons from Corncob with KOH etching plus CO_2 gasification for the adsorption of dyes and phenols from water, Colloids Surf. A 279 (2006) 69–78.
[14] B.H. Hameed, A.T.M. Din, A.L. Ahmad, Adsorption of methylene blue onto bamboo-based activated carbon: kinetics and equilibrium studies, J. Hazard. Mater. 141 (2007) 819–825.

[15] I.A.W. Tan, B.H. Hameed, A.L. Ahmad, Equilibrium and kinetic studies on basic dye adsorption by oil palm fibre activated carbon, Chem. Eng. J. 127 (2007) 111–119.
[16] I.A.W. Tan, B.H. Hameed, A.L. Ahmad, Optimization of preparation conditions for activated carbons from coconut husk using response surface methodology, Chem. Eng. J. 137 (2008) 462–470.
[17] G.N. Manju, C. Raji, T.S. Anirudhan, Evaluation of coconut husk carbon for the removal of arsenic from water, Water Res. 32 (10) (1998) 3062–3070.
[18] J.H. Tay, X.G. Chen, S. Jeyaseelan, N. Graham, Optimising the preparation of activated carbon from digested sewage sludge and coconut husk, Chemosphere 44 (2001) 45–51.
[19] S. Wang, Z.H. Zhu, A. Coomes, F. Haghseresht, G.Q. Lu, The physical and surface chemical characteristics of activated carbons and the adsorption of methylene blue from wastewater, J. Colloid Interface Sci. 284 (2005) 440–446.
[20] G.G. Stavropoulos, A.A. Zabaniotou, Production and characterization of activated carbons from olive-seed waste residue, Microporous Mesoporous Mater. 82 (2005) 79–85.
[21] T.W. Weber, R.K. Chakkravorti, Pore and solid diffusion models for fixed-bed adsorbers, AIChE J. 20 (1974) 228.
[22] F. Haghseresht, G. Lu, Adsorption characteristics of phenolic compounds onto coal-reject-derived adsorbents, Energy Fuels 12 (1998) 1100–1107.
[23] K. Fytianos, E. Voudrias, E. Kokkalis, Sorption–desorption behavior of 2,4-dichloriphenol by marine sediments, Chemosphere 40 (2000) 3–6.
[24] M. Hosseini, S.F.L. Mertens, M. Ghorbani, M.R. Arshadi, Asymmetrical Schiff bases as inhibitors of mild steel corrosion in sulphuric acid media, Mater. Chem. Phys. 78 (2003) 800.
[25] S. Langergren, B.K. Svenska, Zur theorie der sogenannten adsorption geloester stoffe, Veternskapsakad Handlingar 24 (4) (1898) 1–39.
[26] Y.S. Ho, G. McKay, Sorption of dye from aqueous solution by peat, Chem. Eng. J. 70 (1998) 115–124.
[27] W.J. Weber, J.C. S Morris, Proceedings of International Conference on Water Pollution Symposium, vol. 2, Pergamon, Oxford, 1962, pp. 231–266.
[28] D.S. Faust, M.O. Aly, Chemistry of Wastewater Treatment, Butterworths, Boston, 1983.
[29] M. El-Guendi, Homogeneous surface diffusion model of basic dyestuffs onto natural clay in batch adsorbers, Adsorp. Sci. Technol. 8 (2) (1991) 217–225.
[30] T.C. Chandra, M.M. Mirna, Y. Sudaryanto, S. Ismadji, Adsorption of basic dye onto activated carbon prepared from durian shell: studies of adsorption equilibrium and kinetics, Chem. Eng. J. 127 (2007) 121–129.
[31] D. Kavitha, C. Namasivayam, Experimental and kinetic studies on methylene blue adsorption by coir pith carbon, Bioresour. Technol. 98 (2007) 14–21.
[32] F.C. Wu, R.L. Tseng, R.S. Juang, Comparisons of porous and adsorption properties of carbons activated by steam and KOH, J. Colloid Interface Sci. 283 (2005) 49–56.
[33] K. Mohanty, D. Das, M.N. Biswas, Adsorption of phenol from aqueous solutions using activated carbons prepared from *Tectona grandis* sawdust by $ZnCl_2$ activation, Chem. Eng. J. 115 (2005) 121–131.
[34] Y.S. Ho, G. McKay, Pseudo-second order model for sorption processes, Process Biochem. 34 (1999) 451–465.
[35] N. Kannan, M.M. Sundaram, Kinetics and mechanism of removal of methylene blue by adsorption on various carbons—a comparative study, Dyes Pigments 51 (2001) 25–40.